

***New Phytologist* Supporting Information**

Article title: **Plant hydraulics improves and topography mediates prediction of aspen mortality in southwestern USA**

Authors: Xiaonan Tai, D. Scott Mackay, William R. L. Anderegg, John S. Sperry and Paul D. Brooks

Article acceptance date: 10 June 2016

The following Supporting Information is available for this article:

Fig. S1 Monotonic decline of soil moisture during growing season from May to August for the 2000–2003 drought and for the 1979–2009 period across Colorado’s aspen forest based on variable infiltration capacity (VIC) simulated soil water content.

Fig. S2 Simulations used to generate the ensemble of reference curves in sensitivity analysis.

Fig. S3 Sensitivity analysis with respect to values of m and the corresponding explanatory power and regression slope of $\Delta p(\theta_{3D})$ in different topographic areas.

Notes S1 Key processes and parameterizations of TREES.

Fig. S1 Monotonic decline of mean soil moisture during growing season from May to August for the 2000–2003 drought and for the 1979–2009 period across Colorado’s aspen forest based on variable infiltration capacity (VIC) NLDAS-2 soil water product. Error bars represent the standard deviations of simulated soil water content across the landscape.

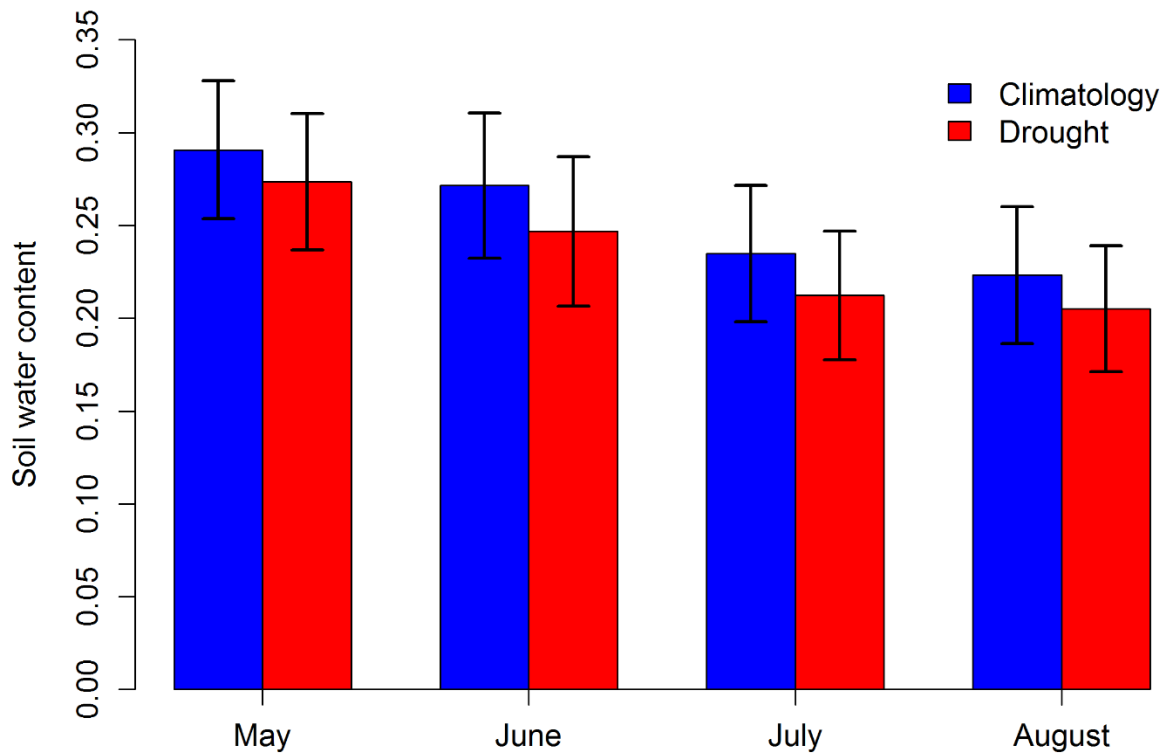


Fig. S2 Simulations used to generate the ensemble of reference curves in the sensitivity analysis.

A total of 27 sets of simulations were carried out for a given initial soil water content and soil texture, with different meteorological time course, VPD magnitude, and soil dry down duration.

(a) Mean and standard deviation of safety loss values at a given initial soil moisture and soil texture. (b) Ensemble of 27 sets of reference curves, each of which corresponds to a specific meteorological time course, VPD magnitude, and soil dry down duration. The R^2 for all fitted curves were greater than 0.9. Three sets of curves with highest, medium, and lowest safety loss at a given soil water content were selected from this ensemble and used to evaluate the influence of uncertainties associated with reference curves in explaining mortality.

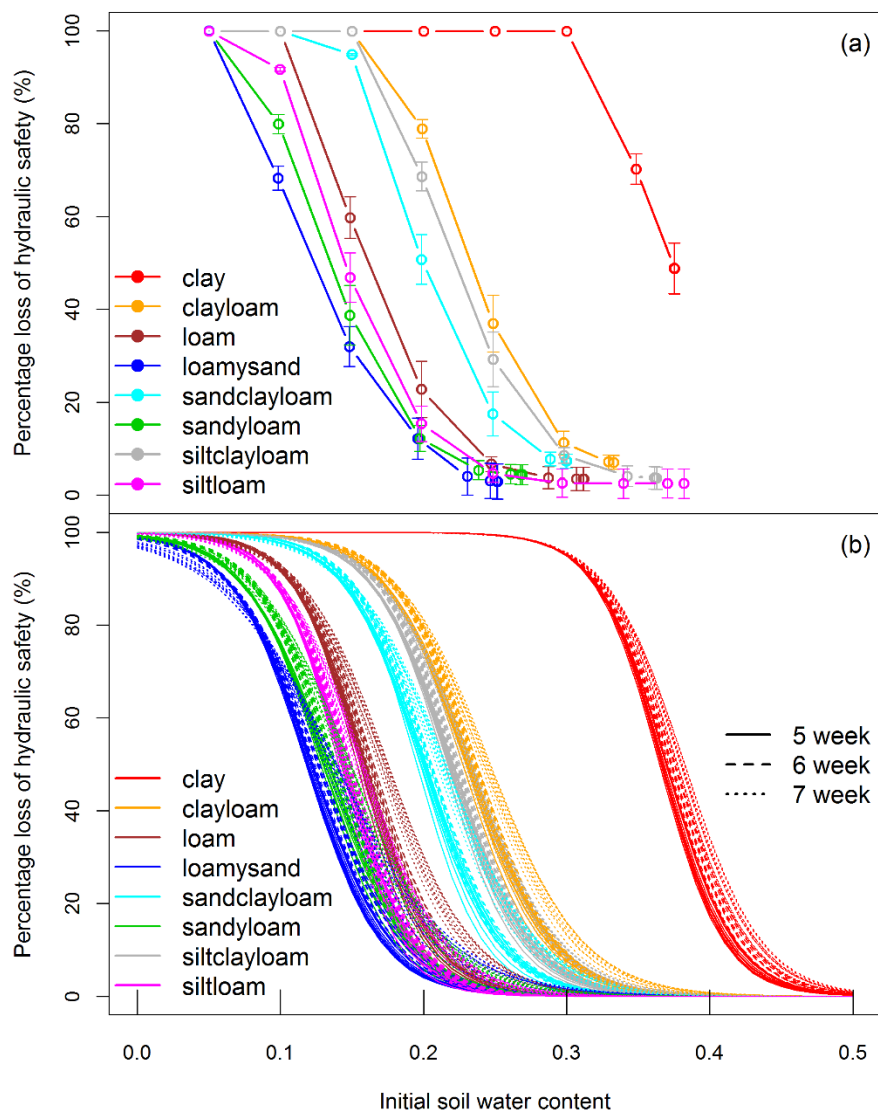
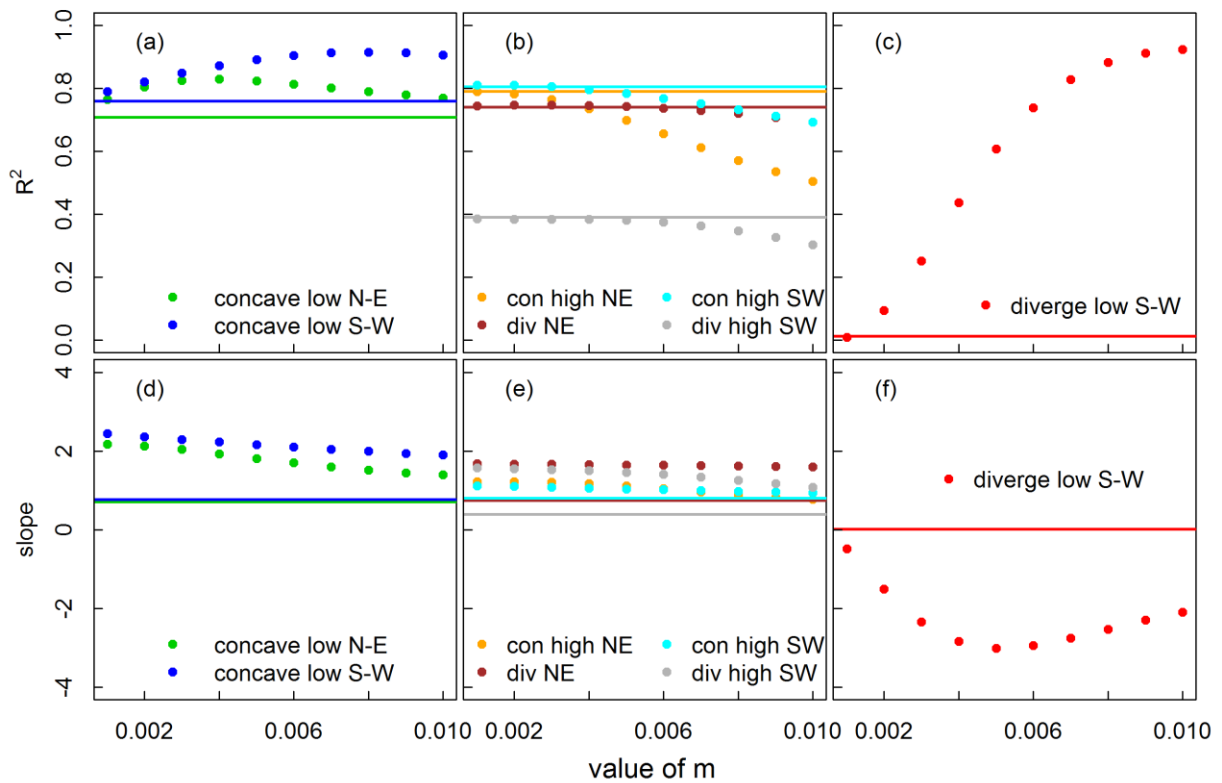


Fig. S3 Sensitivity analysis with respect to values of m and the corresponding explanatory power and regression slope of $\Delta p(\theta_{3D})$ in different topographic categories. Soil moisture from June and a reference curve with medium vulnerability were used. Low and concave areas were shown in (a, d); high elevation regions (including convergent on N–E/S–W, divergent on S–W) or divergent regions on N–E aspect were shown in (b, e); low, divergent and S–W aspect were shown in (c, f). Dots represent 3D and solid lines represent 1D safety loss metrics.



Notes S1 Key processes and parameterizations of TREES.

The Terrestrial Regional Ecosystem Exchange Simulator (TREES) (Mackay *et al.*, 2015) couples photosynthesis, stomatal conductance, and transpiration in a steady state solution at 30-min time steps. Micrometeorological forcing data includes air temperature, wind speed, radiation, vapor pressure deficit, and soil temperature.

TREES explicitly solves soil-plant hydraulics following approaches described in Sperry *et al.* (1998). From Darcy's Law,

$$E = -K(\psi) d\psi/dx \quad \text{Eqn1}$$

where E is the transpiration rate (per leaf area), $d\psi/dx$ is the water potential gradient, and $K(\psi)$ is the hydraulic conductivity expressed per leaf area. In plant tissue, the nonlinear decrease of $K(\psi)$ with more negative ψ is often described by vulnerability curve as in Eqn2.

$$K(\psi) = K_{max} * e^{-\left(\frac{-\psi}{b}\right)^c} \quad \text{Eqn2}$$

where K_{max} is the maximum hydraulic conductivity, which can be derived from the transpiration, predawn and midday leaf water potential at saturated condition. b and c are curve parameters used to describe the sensitivity of K to decreasing Ψ in plant xylem. In soil, the $K(\psi)$ depends largely on soil texture and is determined using van Genuchten formula (Van Genuchten, 1980). Since K decreases nonlinearly with decreasing Ψ due to cavitation in xylem and the displacement of water by air in soil pores, E shows asymptotic increase as Ψ gets more negative. E_{crit} represents the maximum point that E can reach without hydraulic failure while the corresponding K is approaching 0 (Sperry *et al.*, 1998; Manzoni *et al.*, 2013). Key parameters in deriving E_{crit} include vulnerability curve parameters, soil hydraulic parameters, predawn and midday leaf water potential at saturated conditions and saturated hydraulic conductivity.

The whole plant canopy scale stomatal conductance (G_s) was calculated by combining Darcy's Law and Fick's law of diffusion as

$$G_s = K(\psi)(\psi_s - \psi_l)/D \quad \text{Eqn 3}$$

where ψ_l is leaf water potential and ψ_s is soil water potential integrated over the rooting depth of the plant; D is vapor pressure deficit in the canopy. E is solved iteratively until convergence is reached between demand-driven E and supply-driven E (Mackay *et al.*, 2015).

In addition to plant hydraulics, TREES also solves for water balance in soil including soil ponding, infiltration, downward and upward capillary rise, as well as soil evaporation (Mackay *et al.*, 2015). Rooting depth is mainly used to solve soil water balance and update soil water contents.

TREES was parameterized for the healthy aspen stand using vulnerability to cavitation curves from previous studies (Anderegg *et al.*, 2013), and sap flux data to obtain midday transpiration at saturated hydraulic conductivity. Measured predawn and midday water potentials at saturated hydraulic conductivity were also used. Site-specific soil texture data was used to parameterize the soil hydraulic properties (mainly geometric mean particle diameter, and geometric standard deviation of particle size), following methods in (Campbell, 1985). The measured rooting depth was discretized into four layers. The soil water balance was updated in separate layers, using rhizosphere flux rates determined from the plant water balance solution. The same configuration was applied for the SAD stand, except for the transpiration at saturated hydraulic conductivity, as well as predawn and midday water potentials at saturated hydraulic conductivity measured at the SAD stand.

References

- Anderegg WR, Plavcová L, Anderegg LD, Hacke UG, Berry JA, Field CB. 2013.** Drought's legacy: multiyear hydraulic deterioration underlies widespread aspen forest die-off and portends increased future risk. *Global Change Biology* **19**: 1188–1196.
- Campbell GS. 1985.** *Soil physics with BASIC: transport models for soil–plant systems*. Elsevier.
- Mackay DS, Roberts DE, Ewers BE, Sperry JS, McDowell NG, Pockman WT. 2015.** Interdependence of chronic hydraulic dysfunction and canopy processes can improve integrated models of tree response to drought. *Water Resources Research* **51**: 6156–6176.
- Manzoni S, Vico G, Porporato A, Katul G. 2013.** Biological constraints on water transport in the soil–plant–atmosphere system. *Advances in Water Resources* **51**: 292–304.
- Sperry J, Adler F, Campbell G, Comstock J. 1998.** Limitation of plant water use by rhizosphere and xylem conductance: results from a model. *Plant, Cell & Environment* **21**: 347–359.
- Van Genuchten MT. 1980.** A closed-form equation for predicting the hydraulic conductivity of unsaturated soils. *Soil Science Society of America Journal* **44**: 892–898.